Available online at www.sciencedirect.com

SciVerse ScienceDirect

Journal of Electrocardiology 45 (2012) 478–484

JOURNAL OF Electrocardiology

www.jecgonline.com

Evaluation of the electrocardiogram in identifying and quantifying lateral involvement in nonanterior wall infarction using cardiovascular magnetic resonance imaging☆,☆☆

Kirian van der Weg, MD,[a,*] Sebastiaan C.A.M. Bekkers, MD, PhD,[b] Bjorn Winkens, PhD,[c] Miguel E. Lemmert, MD,[d] Simon Schalla, MD,[b] Harry J.G.M. Crijns, MD, PhD,[d] Johannes Waltenberger, MD, PhD,[e] Anton P.M. Gorgels, MD, PhD[d]

[a]*Maastricht University, AZ Maastricht, The Netherlands*
[b]*Maastricht University Medical Centre, AZ Maastricht, The Netherlands*
[c]*Department of Methodology and Statistics, Maastricht University, AZ Maastricht, The Netherlands*
[d]*Cardiovascular Institute Maastricht, Maastricht University Medical Centre, AZ Maastricht, The Netherlands*
[e]*Department für Kardiologie und Angiologie, Universitätsklinikum Münster, Germany*

Received 1 August 2011

Abstract

Purpose: The objective of this study was to assess the involvement and extent of lateral wall myocardial infarction (MI) in patients with a first nonanterior wall MI, as reflected by changes in precordial leads. Delayed enhancement cardiac magnetic resonance imaging was used as a gold standard to localize and quantify myocardial scar tissue.

Methods: Electrocardiogram and cardiac magnetic resonance were studied in 56 patients. Areas involved were related to QRS changes in precordial leads.

Results: Significant correlations were found between lateral wall involvement and R waves in V_1 and V_6 (P = 0.009-0.022). For patients with circumflex branch occlusions, the MI size of the apical and lateral segments correlated strongly with the characteristics of R waves in V_1 and V_2 (P = 0.001-0.034).

Conclusions: Tall and broad R waves in V_1 reflect lateral wall MI, especially in circumflex occlusions.

Keywords: Electrocardiography; Ischemia; Myocardial infarction; Magnetic resonance imaging

Introduction

Myocardial infarction (MI) can be reflected in the standard 12-lead surface electrocardiogram (ECG) as a loss of R waves and/or formation of Q waves in leads with positive poles facing the necrotic myocardial wall. In nonanterior MI, this is typically represented in leads II, III, aVF, V_5, and V_6. In addition, a gain in height and width of R waves in V_1 has been observed as a result of necrosis in the myocardial area opposite to its positive electrode.[1-3] Some authors reported a correlation between tall R waves in V_1 with lateral wall MI.[4-7] However, to our knowledge, little is known regarding the height of the R waves in lead V_1 as a quantitative marker for the extent of MI size without the use of other ECG characteristics.

Because of its excellent spatial resolution and possibility to image in any anatomical orientation, delayed enhancement cardiac magnetic resonance imaging (DE-CMR) has become the clinical gold standard to determine localization and extent of MI.[8,9] It has also shown its quality in correlating ECG findings and MI location and size.[8,10]

In this study, we sought to quantitatively test the hypothesis that the changes in the QRS complex in V_1 and V_6 are related to lateral involvement, in an independent cohort of consecutive cases with a nonanterior MI. If correct, these findings are not only of importance to appropriately classify MI location but also have clinical implications in

☆ Funding sources: The MAST project was supported by a grant from the MUMC+ research fund.

☆☆ Disclosures: No disclosures to be reported.

* Corresponding author. Department of Cardiology, Maastricht School of Cardiovascular Diseases, Maastricht University Medical Centre, P Debyelaan 25, 6229 HX Maastricht, PO Box 5800, 6202 AZ Maastricht, The Netherlands.

E-mail address: kirian.vander.weg@mumc.nl

0022-0736
doi:10.1016/j.jelectrocard.2012.04.008

identifying patients with extensive lateral wall involvement and at high risk for papillary muscle infarction.

Methods

Patient population

Consecutive patients were studied, presenting with a first acute nonanterior wall ST-elevation MI (STEMI) at Maastricht University Medical Center from August 2006 to March 2008. *ST-elevation MI* was defined according to ECG and enzymatic criteria according to the recently published consensus.[11] *Nonanterior* was defined as the culprit artery being either the circumflex (CX), the right coronary artery (RCA), or one of their branches.

Inclusion criteria were (1) symptoms consistent with an acute STEMI lasting for more than 30 minutes but less than 6 hours, (2) ST-elevation of more than 1 mm in anatomically adjacent leads in the initial ECG, (3) occlusion of either the RCA or CX, and (4) availability of CMR images. Exclusion criteria were (1) age below 18 years, (2) cardiogenic shock, (3) pregnancy, (4) inability to obtain informed consent, (5) standard contraindications for CMR, (6) occlusion of the left anterior descending artery, and (7) the presence of a bundle-branch block.

All patients were treated with standard medical care for acute MI and primary percutaneous coronary intervention (PCI) of the culprit artery. The *culprit artery* was defined by the interventional cardiologist based on standard operating procedures using the European Society of Cardiology (ESC) guidelines: irregular borders, eccentricity, ulcerations, and filling defect suggestive of intraluminal thrombi.

The study protocol was approved by the review board of our institution, and informed consent was obtained in all patients.

Cardiovascular magnetic resonance imaging protocol

Cardiovascular magnetic resonance imaging was performed on a 1.5-T Philips Intera scanner (Philips Medical Systems, Best, The Netherlands). Images were acquired using ECG gating, during multiple breath-holds, and using a dedicated 5-element phased array surface coil. Delayed enhancement images were obtained 10 minutes after the

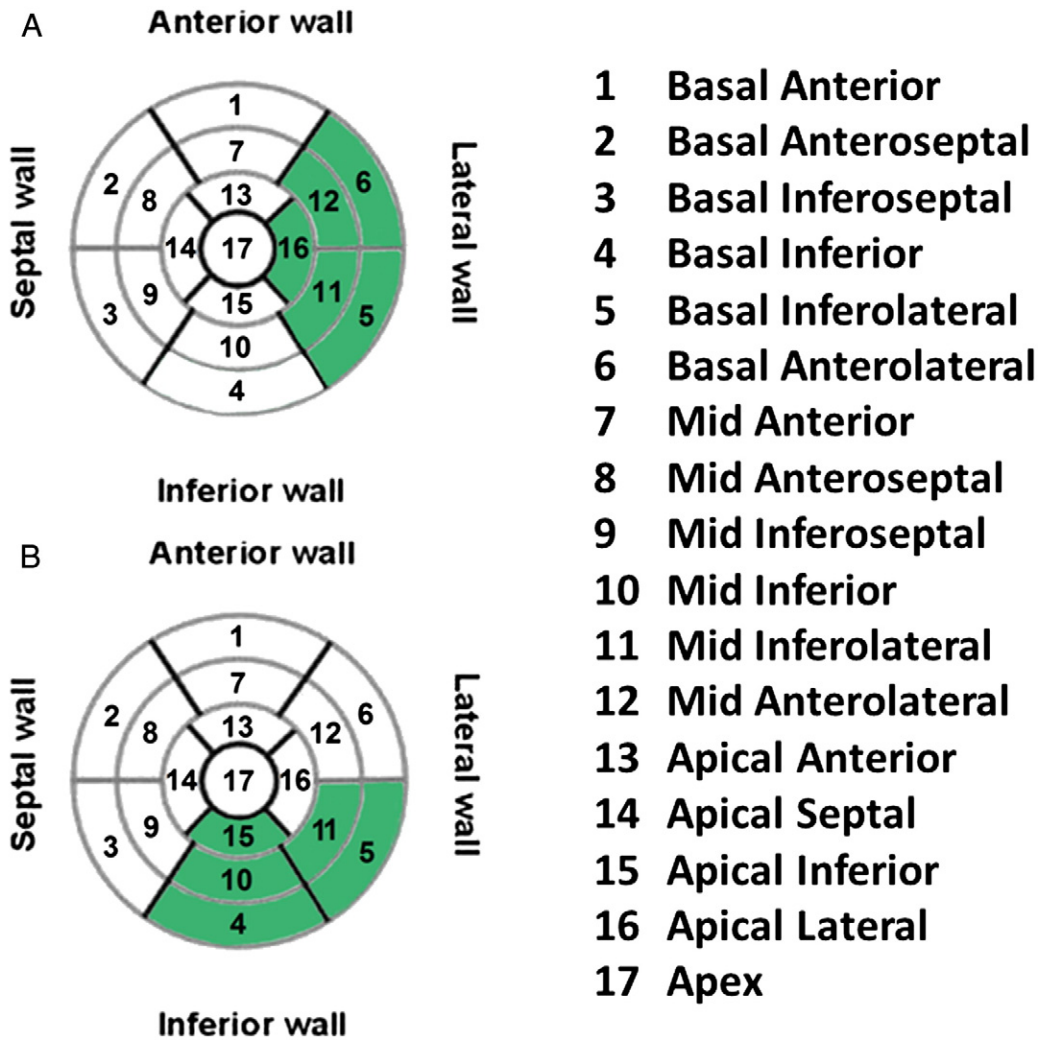

Fig. 1. Bull's-eye model according to the AHA 17 segment model within the highlighted areas in A (the lateral wall) and in B (the inferolateral wall). Color illustration online.

intravenous administration of 0.2 mmol/kg body weight gadolinium-diethylenetriaminepentaacetic acid (Gd-DTPA; Magnevist, Schering, Germany) in short-axis view using a 3-dimensional inversion recovery gradient-echo sequence completely covering the left ventricle (LV) (average TR/TE, 3.9/2.4 milliseconds; flip angle, 15°; matrix, 1.56 × 1.56 mm; reconstructed slice thickness, 6 mm). Immediately before the delayed enhancement images, a Look-Locker sequence was run at to find the inversion time (typical range, 200-280 milliseconds) that optimally suppressed the signal of noninfarcted myocardium.

Cardiac magnetic resonance image analysis

Delayed enhancement cardiac magnetic resonance images were analyzed off-line independently by a single experienced observer, blinded to the clinical and ECG data, using commercially available software (CAAS MRV 3.0; Pie Medical Imaging, Maastricht, The Netherlands). Endocardial and epicardial contours were manually traced on the DE-CMR images. Final left ventricular MI size was quantified using an signal intensity (SI) threshold of greater than 5 SD above a remote noninfarcted region and expressed as a percentage of total LV mass.[12] Areas of microvascular obstruction (central hypoenhancement within hyperenhanced area) were included in MI size assessment.

The nomenclature of the American Heart Association (AHA) was used to identify left ventricular wall location of MI.[13] In addition, regional MI size was calculated for the lateral wall (involving segments 5, 6, 11, 12, and 16) and inferolateral wall (involving segments 4, 5, 10, 11, and 15) by summing MI size in these segments and dividing it by the total number of segments per region. The segmental nomenclature follows the AHA 17 segment model (Fig. 1).[13] The inferolateral wall consisted of the inferior wall segments and the inferior segments of the lateral wall.

Electrocardiographic evaluation

Standard 12-lead ECGs were recorded using a General Electric (GE) MAC 5500 12-lead recorder, produced in Freiburg, Germany. Electrocardiogram were analyzed by a single investigator, blinded to clinical and CMR data. The ECG closest to the day of CMR imaging during admission was used for ECG evaluation. This ECG was scanned into a software environment and magnified 8 times. After magnification, the height and width of the Q, R, and S waves in V_1 through V_6 were measured manually. These measurements were used to also calculate the R/S ratio in V_1[5,14] and combined the value of the height and width of the R wave in V_1 by multiplying both, which we termed *surface of R* (although it was not divided by the constant 2) (Fig. 2). Measurements were displayed in mm, with 1 mm corresponding with 40ms for width and with 0.1 mV for height.

Table 1
Patient characteristics

Variable	Total (n = 56)	
	No. of patients	%
Male	41	73
Diabetes mellitus	4	7
Hypertension	18	33
Dyslipidemia	18	33
Smokers or a history of smoking	51	91
Positive family history	24	44
Peripheral artery disease	6	11
AP in preceding 24 h	25	45
Baseline TIMI 0-1 flow[a]	39	72
Final TIMI 3 flow[a]	50	93
RCA occlusion	45	80
CX occlusion	11	20
Multiple vessel disease[a]	27	49
Variable	**Mean**	**SD**
Age (y)	58	10
Total minutes of ischemia[b]	213	71
LVIS (%)	12	8
RIS lateral wall (%)	9	14
RIS inferolateral wall (%)	22	15
CK-MB t = 0 h (mg/L)	7	6
CK-MB t = 6 h (mg/L)	171	155
Troponin-T t = 0 h (μg/L)	0.05	0.11
Troponin-T t = 6 h (μg/L)	4.2	3.8
CRP t = 0 h (mg/L)	5.0	8.4
Pro-BNP t = 48 h (pmol/L)	110	93

Normal values: CK-MB male, <4.9 mg/L; female, <2.9 mg/L; troponin T, <0.01 μg/L; CRP, <10 mg/L, Pro-BNP, <35 pmol/L.
AP indicates angina pectoris; RCA, right coronary artery; CX, circumplex; SD, standard deviation; LVIS, left ventricular infarct size; RIS, regional infarct size.
[a] Data from angiography.
[b] Calculated as time from onset of symptoms until intervention.

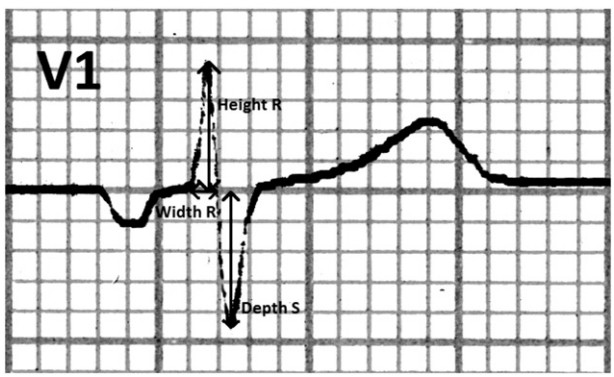

Fig. 2. Electrocardiogram measurement. Image showing the method of measuring the QRS variables in lead V_1.

Statistical and data analyses

Electrocardiographic characteristics were correlated with MI size of each single inferior and lateral segment (Fig. 1) and with the lateral and inferolateral wall (as described above). A subgroup analysis was applied for RCA and CX MI separately. Simple linear regression was used to assess the effects of characteristics of R and Q waves on regional MI size of the lateral and inferolateral wall. In addition, these effects were assessed by multiple linear regression with correction for the most significant patient characteristics with a maximum of 4 because of a total sample size of 56 patients. The goodness-of-fit of the model was displayed by R^2, the square number of the correlation coefficient. The correlation

of nonnormally distributed data, determined by histograms and qq-plots, was evaluated using Kendall or Spearman correlations (r_s). Correlations were regarded as significant if $P \leq .05$. Data were analyzed using SPSS version 16.0 (IBM, New York). Because of the extent of the data section, only relevant correlations will be presented in the result section, focusing on leads V_1, V_2, and V_6.

Results

The baseline characteristics are shown in Table 1. In total, 56 consecutive patients with a mean age of 58 years (SD, 10 years; range, 31-81 years) were included in this study. The culprit artery was the RCA in 46 (82%) and the CX in 10 (18%) patients. Patients underwent a CMR study 5 (SD, 2; range, 2-12) days after admission and intervention. The target ECG was recorded within a mean of 3 (SD, 2; range, 0-11) days before CMR study. Thirty-nine patients (72%) had thrombolysis in myocardial infarction (TIMI) flow grade 0 to 1 before PCI, and TIMI 3 was established in 50 patients (93%) after PCI. Multivessel disease was present in 27 (49%).

Electrocardiogram variables studied in relation to the lateral wall

Simple linear regression analyses showed a moderate correlation between regional MI size of the lateral wall and the height, width, and surface area of R waves and R/S ratio in V_1 and a negative correlation with the height of R waves in V_6 (Table 2). The highest correlation was found for the R/S ratio and surface of R in V_1 and the height of R waves in V_6. All had a P value of .001.

Multiple linear regression analyses showed a high correlation when corrected for potential confounders of sex, occluded vessel (RCA or CX), and single or multiple vessel disease. All regression models had a P value of less than .001. The most significant associations were found for the surface of R in V_1 ($p = 0.010$) and the height of R waves in V_6 ($P = 0.009$). R waves in V_2 were found to have little value in evaluating the extent of lateral wall involvement (Fig. 3).

Electrocardiogram variables studied in relation to the inferolateral wall

As shown in Table 2, a moderate correlation was found between regional MI size of the inferolateral

Fig. 3. Electrocardiographic and CE-CMR images of a large lateral infarct. Top, 12-lead ECG showing Q waves in leads II, III, aVF, and V_6, a tall R wave in V_1, and loss of height of R in V_6. Right, CE-CMR images showing an inferolateral and lateral wall infarction (between white arrows) with microvascular obstruction (see black arrow).

segments and the depth and width of Q waves in V_6. Multiple linear regression slightly improved the correlation of these characteristics.

Apical inferior and apical lateral segments in CX occlusion

The ECG characteristics of and the MI size of individual segments showed a clear association for the apical inferior segment (segment 15) and the apical lateral segment (segment 16) in the total population. In the 11 patients with CX occlusion, Spearman test showed a strong correlation between the MI size in segment 15 and segment 16 and the height, width, and surface of R waves and R/S ratio in V_1 and the height and width of R waves in V_2. The surface of R waves in V_1 had the highest correlations with the apical inferior and apical lateral segment (r_s = 0.98, P < .001 and r_s = 0.82, P = .002, respectively) (Table 3).

Discussion

The principal findings of this study are (1) tall or wide R waves in V_1 or small R waves in V_6 are quantitatively associated with a lateral MI, (2) the depth and width of Q waves in V_6 corresponded best with inferolateral MI, and (3) very strong relations were found between the apical inferior or apical lateral segment and the height and width of R waves in V_1 or V_2 as a result of occlusion of the CX.

Table 2
Simple and multiple linear regression analyses

Simple and multiple linear regression analyses for regional infarct size of the lateral wall

	R	B	95% CI	*P*
Simple linear regression				
Height of R in V_1 in mm	0.41	4.57	1.77 to 7.38	.003
Width of R in V_1 in mm	0.33	15.94	3.59 to 28.28	.012
Surface of R in V_1 in mm^2	0.43	4.62	1.94 to 7.29	.001
R/S in V_1	0.43	13.87	5.93 to 21.81	.001
Height of R in V_2 in mm	0.18	0.70	−0.35 to 1.74	.188
Width of R in V_2 in mm	0.10	4.91	−9.29 to 19.11	.491
Height of R in V_6 in mm	0.46	-1.31	−2.01 to −0.60	.001
Multiple linear regression				
Height of R in V_1 in mm	0.68	3.50	0.82 to 6.18	.011
Width of R in V_1 in mm	0.67	15.58	2.39 to 28.77	.022
Surface of R in V_1 in mm^2	0.68	3.44	0.87 to 6.01	.010
R/S in V_1	0.65	6.96	−0.75 to 14.67	.076
Height of R in V_2 in mm	0.65	0.83	−0.07 to 1.73	.069
Width of R in V_2 in mm	0.65	9.79	−2.52 to 22.09	.116
Height of R in V_6 in mm	0.65	-0.92	−1.60 to −0.25	.009

Simple and multiple linear regression analyses for regional infarct size of the inferolateral wall

	R	B	95% CI	*P*
Simple linear regression				
Depth of Q in V_6 in mm	0.33	6.39	1.26-11.530	.016
Width of Q in V_6 in mm	0.36	18.67	5.30-32.04	.007
Multiple linear regression				
Depth of Q in V_6 in mm	0.38	6.77	1.04-12.50	.022
Width of Q in V_6 in mm	0.40	19.30	3.92-34.69	.015

Confounders in multiple regression are sex, occluded vessel, and single or multiple vessel disease. Sex was found to be an independent confounder. All multiple correlation models of the lateral wall had a P < .001, the multiple correlation models of the inferolateral wall had a P < .042 and .032, respectively. P values in table correspond with B value. R indicates correlation value; B, the increase of infarct in percentage when the variable increases with 1.00; CI, confidence interval.

Table 3
Spearman correlation for the apical inferior and lateral segments in CX occlusion

Spearman correlation for the apical inferior and lateral segments

	Segment 15		Segment 16	
	r_s	*P*	r_s	*P*
Height of R in V_1 in mm	0.81	.002	0.80	.003
Width of R in V_1 in mm	0.56	.046	0.60	.034
Surface of R in V_1 in mm^2	0.98	<.001	0.82	.002
R/S ratio in V_1	0.90	<.001	0.77	.005
Height of R in V_2 in mm	0.87	.001	0.77	.005
Width of R in V_2 in mm	0.91	<.001	0.76	.006

Segment 15 is the apical inferior segment. Segment 16 is the apical lateral segment.

The R in V_1 and V_2

The clinical significance of the tall R waves in V_1 has recently been reported by Bayes de Luna et al and Rovai et al.[6,15-17] Our finding of tall R waves in V_1 being correlated with lateral wall MI instead of the posterior wall MI was congruent with their results. However, their findings were observational and based on small study populations that did not allow quantitative analysis. Our population is larger, enabling quantification of the relation between the characteristics of R waves in V_1 or V_2 and the extent of lateral MI using multivariate regression analysis.

A well-validated method for quantifying MI size with ECG characteristics is the Selvester score. This scoring system predicts MI size and location using 50 criteria. To accurately predict MI size, all 50 criteria should be evaluated and scored. Recent studies correlating Selvester score with MI size determined by CMR showed that the score was more accurate in predicting anterior vs nonanterior infarct size with R equal to 0.13 to 0.78,[18-23] with most results approximately R = 0.6. Using 1 single criterion, our data showed correlations of R = 0.65 to 068 when corrected for sex, occluded vessel, and single or multivessel disease. This feature could provide a faster method for determining lateral infarct size, although studies in other and larger populations are needed to confirm the correlations found.

Changes of the QRS complex in lead V_6

Loss of height of R waves in lead V_6 was found to be a sign of a lateral MI and was quantitatively related to MI size. Q waves in V_6, however, were related to inferolateral involvement. In the literature, deep and wide Q waves in V_6 are classically[24-26] as well according to the Selvester criteria[5,7] associated with a lateral MI. Our findings suggest a more specific correlation, that is, inferolateral involvement. This is supported by other studies reporting poor correlations between deep or wide Q waves in V_6 and the lateral wall.[2,17] The fact that Q waves and the loss of height of R waves in V_6 correspond to different locations involved may be explained

by the activation sequence of the inferior wall being activated before the lateral wall.[27]

R wave behavior in CX occlusion

R waves were on average higher in patients with a CX occlusion. This indicates that tall R waves in V_1 are mostly due to occlusion of the CX, as expected considering its supply area. In particular, high correlations were found between tall or broad R waves in V_1 or V_2 and the apical inferior or lateral segment in patients with a CX occlusion. This finding has, to our knowledge, not previously been described. Apparently in this subpopulation of occlusion of dominant CXs leading to STEMI with ST elevation in leads II, III, and aVF, the vectors of V_1 and V_2 are more apically oriented.

Limitations of this study

Our study included nonanterior STEMI patients. Including only STEMI cases led to an underrepresentation of CX occlusions and to the selection of dominant CX occlusions. It is therefore not known, whether our findings in predicting MI size are also applicable to non-STEMI populations. Another limitation is the relatively small study population of patients with CX occlusion.

Clinical implications

Our findings give insight into the involvement of LV segments in relation to the changes in the precordial leads in lateral and inferolateral wall MI. Our data confirm previous observations that tall or broad R waves in V_1 are correlated with lateral wall MI instead of posterior MI. In addition to above, our findings have important clinical implications in identifying extensive involvement of the lateral wall. Lateral wall MI could be associated with papillary muscle MI and presence of both identifies patients at risk for mitral regurgitation.[28]

Summary and conclusion

These data represent, to our knowledge, the largest group of nonanterior MI patients quantitatively analyzed for ECG characteristics in the precordial leads and MI size and location using CMR. Characteristics of R and S waves studied in lead V_1 indicate lateral wall involvement and give insight in the extent of infarct size. Depth and width of Q waves in V_6 are related to an inferolateral location and infarct size.

Acknowledgments

The art work of Geert-Jan van Zonneveld is highly appreciated.

References

1. Brady WJ, Erling B, Pollack M, Chan TC. Electrocardiographic manifestations: acute posterior wall myocardial infarction. J Emerg Med 2001;20:391.
2. Moon JC, De Arenaza DP, Elkington AG, et al. The pathologic basis of Q-wave and non-Q-wave myocardial infarction. JACC 2004;44:554.
3. Myers GB, Klein HA, Hiratzka T. Correlation of electrocardiographic and pathologic findings in posterior infarction. Am Heart J 1948;38:547.
4. Bough E, Boden W, Korr K, Gandsman E. Left ventricular asynergy in electrocardiographic "posterior" myocardial infarction. J Am Coll Cardiol 1984;4:209.
5. Ward RM, White RD, Ideker RE, et al. Evaluation of a QRS scoring system for estimating myocardial infarct size. IV. Correlation with quantitative anatomic findings for posterolateral infarcts. Am J Cardiol 1984;53:706.
6. Bayes de Luna A, Wagner G, Birnbaum Y, et al. A new terminology for left ventricular walls and location of myocardial infarcts that present Q wave based on the standard of cardiac magnetic resonance imaging: a statement for healthcare professionals from a committee appointed by the International Society for Holter and Noninvasive Electrocardiography. Circulation 2006;114:1755.
7. Horacek BM, Warren JW, Albano A, et al. Development of an automated Selvester Scoring System for estimating the size of myocardial infarction from the electrocardiogram. J Electrocardiol 2006;39:162.
8. Kim HW, Farzaneh-Far A, Kim RJ. Cardiovascular magnetic resonance in patients with myocardial infarction: current and emerging applications. J Am Coll Cardiol 2009;55:1.
9. Wagner A, Mahrholdt H, Holly TA, et al. Contrast-enhanced MRI and routine single photon emission computed tomography (SPECT) perfusion imaging for detection of subendocardial myocardial infarcts: an imaging study. Lancet 2003;361:374.
10. Engblom H, Hedström E, Heiberg E, Wagner GS, Pahlm O, Arheden H. Size and transmural extent of first-time reperfused myocardial infarction assessed by cardiac magnetic renonance can be estimated by 12 -lead electrocardiogram. Am Heart J 2005;150:920.
11. Thygesen K, Alpert JS, White HD. Infarction. JEAAWTFftRoM. Universal definition of myocardial infarction. J Am Coll Cardiol 2007;50:2173.
12. Bondarenko O, Beek AM, Hofman MB, et al. Standardizing the definition of hyperenhancement in the quantitative assessment of infarct size and myocardial viability using delayed contrast-enhanced CMR. J Cardiovasc Magn Reson 2005;7:481.
13. Cerqueira MD, Weissman NJ, Dilsizian V, et al. Standardized myocardial segmentation and Nomenclature for tomographic imaging of the heart. Circulation 2002;105:539.
14. Perloff JK. The recognition of strictly posterior myocardial infarction by conventional scalar electrocardiography. Circulation 1964;30:706.
15. Bayes de Luna A, Cino JM, Pujadas S, et al. Concordance of electrocardiographic patterns and healed myocardial infarction location detected by cardiovascular magnetic resonance. Am J Cardiol 2006;97:443.
16. Bayes de Luna A, Zareba W. New terminology of the cardiac walls and new classification of Q-wave M infarction based on cardiac magnetic resonance correlations. Ann Noninvasive Electrocardiol 2007;12:1.
17. Rovai D, Di Bella G, Rossi G, et al. Q-wave prediction of myocardial infarct location, size and transmural extent at magnetic resonance imaging. Coron Artery Dis 2007;18:381.
18. Bang LE, Ripa RS, Grande P, Kastrup J, Clemmensen PM, Wagner GS. Comparison of infarct size changes with delayed contrast-enhanced magnetic resonance imaging and electrocardiogram QRS scoring during the 6 months after acutely reperfused myocardial infarction. J Electrocardiol 2008;41:609.
19. Geerse DA, Wu KC, Gorgels AP, Zimmet J, Wagner GS, Miller JM. Comparison between contrast-enhanced magnetic resonance imaging and Selvester QRS scoring system in estimating changes in infarct size between the acute and chronic phases of myocardial infarction. Ann Noninvasive Electrocardiol 2009;14:360.
20. Knippenberg SA, Wagner GS, Ubachs JF, et al. Consideration of the impact of reperfusion therapy on the quantitative relationship between the Selvester QRS score and infarct size by cardiac MRI. Ann Noninvasive Electrocardiol 2010;15:238.
21. Weir RA, Martin TN, Murphy CA, et al. Comparison of serial measurements of infarct size and left ventricular ejection fraction by

contrast-enhanced cardiac magnetic resonance imaging and electrocardiographic QRS scoring in reperfused anterior ST-elevation myocardial infarction. J Electrocardiol 2010;43:230.
22. Rovers WC, van Boreen MC, Robinson M, et al. Comparison of the correlation of the Selvester QRS scoring system with cardiac contrast-enhanced magnetic resonance imaging-measured acute myocardial infarct size in patients with and without thrombolytic therapy. J Electrocardiol 2009;42:139.
23. Engblom H, Wagner GS, Setser RM, et al. Quantitative clinical assessment of chronic anterior myocardial infarction with delayed enhancement magnetic resonance imaging and QRS scoring. Am Heart J 2003;146:359.
24. Friedman H. Diagnostic Electrocardiography and Vectorcardiography. New York: McGraw-Hill; 1985.
25. Gorgels AP, Engelen DJ, Wellens HJJ. The electrocardiogram in acute myocardial infarction. In: Fuster V, editor. Hurst's the Heart. 10th ed. New York: Mcgraw-Hill; 2000.
26. Wagner G. Marriot's electrocardiography. 10th ed. Philadelphia: Lippencott Williams and Wilkins; 2001.
27. Durrer D, van Dam RT, Freud GE, Janse MJ, Meijler FL, Arzbaecher RC. Total excitation of the isolated human heart. Circulation 1970;41:899.
28. Agricola E, Oppizzi M, Pisani M, Meris A, Maisano F, Margonato A. Ischemic mitral regurgitation: mechanisms and echocardiographic classification. Eur J Echocardiogr 2008;9:207.